Inorganic Chemistry

ARTICLE

pubs.acs.org/IC

Theoretical Investigation into the Mechanism of Reductive Elimination from Bimetallic Palladium Complexes

Alireza Ariafard,[†,‡] Christopher J. T. Hyland,[†,§] Allan J. Canty,[*,†] Manab Sharma,[†] and Brian F. Yates[*,†]

[†]School of Chemistry, University of Tasmania, Private Bag 75, Hobart, Tasmania 7001, Australia
[‡]Department of Chemistry, Faculty of Science, Central Tehran Branch, Islamic Azad University, Shahrak Gharb, Tehran, Iran
[§]Department of Chemistry and Biochemistry, California State University, Fullerton, California 92831, United States

S *Supporting Information*

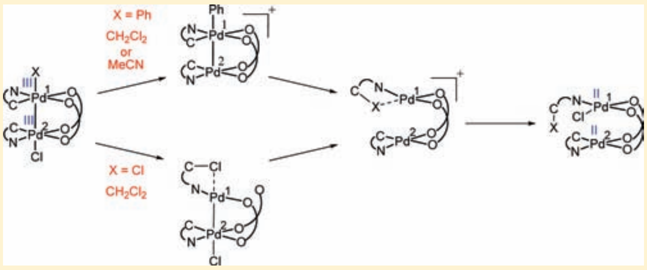

ABSTRACT: Reductive elimination of C−Cl and C−C bonds from binuclear organopalladium complexes containing Pd−Pd bonds with overall formal oxidation state +III are explored by density functional theory for dichloromethane and acetonitrile solvent environments. An X-ray crystallographically authenticated neutral complex, $[(L\text{-}C,N)ClPd(\mu\text{-}O_2CMe)]_2$ (L = benzo[*h*]quinolinyl) (**I**), is examined for C−Cl coupling, and the proposed cation, $[(L\text{-}C,N)PhPd^1(\mu\text{-}O_2CMe)_2Pd^2(L\text{-}C,N)]^+$ (**II**), examined for C−C coupling together with $(L\text{-}C,N)PhPd^1(\mu\text{-}O_2CMe)_2Pd^2Cl(L\text{-}C,N)$ (**III**) as a neutral analogue of **II**. In both polar and nonpolar solvents, reaction from **III** via chloride dissociation from Pd^2 to form **II** is predicted to be favored. Cation **II** undergoes Ph−C coupling at Pd^1 with concomitant Pd^1−Pd^2 lengthening and shortening of the Pd^1−O bond trans to the carbon atom of L; natural bond orbital analysis indicates that reductive coupling from **II** involves depopulation of the $d_{x^2-y^2}$ orbital of Pd^1 and population of the d_{z^2} orbitals of Pd^1 and Pd^2 as the Pd−Pd bond lengthens. Calculations for the symmetrical dichloro complex **I** indicate that a similar dissociative pathway for C−Cl coupling is competitive with a direct (nondissociative) pathway in acetonitrile, but the direct pathway is favored in dichloromethane. In contrast to the dissociative mechanism, direct coupling for **I** involves population of the $d_{x^2-y^2}$ orbital of Pd^1 with Pd^1−O^1 lengthening, significantly less population occurs for the d_{z^2} orbital of Pd^1 than for the dissociative pathway, and d_{z^2} at Pd^2 is only marginally populated resulting in an intermediate that is formally a Pd^1(I)-Pd^2(III) species, $(L\text{-}Cl\text{-}N,Cl)Pd^1(\mu\text{-}O_2CMe)Pd^2Cl(O_2CMe)(L\text{-}C,N)$ that releases chloride from Pd^2 with loss of Pd(I)−Pd(III) bonding to form a Pd(II) species. A similar process is formulated for the less competitive direct pathway for C−C coupling from **III**, in this case involving decreased population of the d_{z^2} orbital of Pd^2 and strengthening of the Pd(I)−Pd(III) interaction in the analogous intermediate with η^2-coordination at Pd^1 by L-Ph-*N*, C^1-C^2.

INTRODUCTION

We have recently reported computational studies of the structures of binuclear organopalladium(III) species **2** (C∼N = L^1, X = Y = Cl) and related cations **3** (C∼N = L^1) (Figure 1).[1] This work follows reports of the synthesis of **2** (C∼N = L^1; X = Y = Cl, O∼O = O_2CMe) from **1**,[2] X-ray structural analyses of **2**,[2] and the proposal that spectroscopically undetected **3** (X = Ph, C∼N = L^2) is an intermediate in the catalytic reaction of 3-methyl-2-phenylpyridine (L^2-H) with $IPh(Mes)(BF_4)$ in acetic acid to form the C−C coupled product L^2-Ph.[3] The computational studies are supportive of the presence of cation **3** in preference to species related to **2** containing an additional donor to Pd^2, for example, as the σ-donor ability of X increases above that of the relatively weak donor Cl in **2** (C∼N = L^1, Y = Cl), the Pd−Cl bond weakens and, in donor solvents such as MeCN, chloride is expected to be liberated.[1] We report here a computational study of C−C reductive elimination from cation **3** (C∼N = L^1, X = Ph) to further examine the chemistry of this class of complex and, in view of the recent computational study of reductive elimination from symmetrical **2** (C∼N = L^1, X = Y = Cl) computed for CH_2Cl_2 as solvent,[2c] we have extended this study to include the neutral species **2** (X = Ph, Y = Cl) and re-examined elimination from **2** (X = Y = Cl) in both CH_2Cl_2 and MeCN environments. The latter results are supportive of the recent mechanistic study[2c] and indicate the presence of a competing dissociative pathway in polar media.

COMPUTATIONAL DETAILS

Gaussian 09[4] was used to fully optimize all the structures reported in this paper at the M06[5] level of density functional theory (DFT). The choice of the M06 functional is based on the fact that this method is capable of considering the medium range π−π stacking interactions in the bimetallic complexes and also of giving a reliable description of the relative energies in some transition-metal systems.[6] The effective core potential of Hay and Wadt with a triple-ξ valence basis set (LANL2TZ) was chosen to describe Pd.[7] The 6-31G(d) basis set was used for other

Received: November 20, 2010
Published: June 14, 2011

atoms.[8] A polarization function of $\xi_f = 1.472$ was also added to Pd.[9] This basis set combination will be referred to as BS1. Frequency calculations were carried out at the same level of theory as for structural optimization. To further refine the energies obtained from the M06/BS1 calculations, we carried out single point energy calculations for all the structures with a larger basis set (BS2). BS2 utilizes the quadruple-ζ valence def2-QZVP[10] basis set on Pd along with the corresponding ECP and the 6-311+G(2d,p) basis set on other atoms. The solvation energies were calculated using BS2 on gas phase optimized geometries with the CPCM solvation model[11] using dichloromethane and acetonitrile as solvents. To estimate the corresponding Gibbs free energies in solvents, ΔG, entropy corrections were calculated at the gas phase M06/BS1 level and added to the solvent potential energies.[12] To provide a more precise dissociation energy for the Pd−Cl bond, basis set superposition errors (BSSE) were evaluated.

To further assess the relative energies derived from the M06 calculations, we also performed B97D[13]/BS2//M06/BS1 single point calculations using the geometries derived from the M06/BS1 calculations with solvent effects included for CH_2Cl_2 and MeCN (see Figures S1 and S2 in the Supporting Information). We also optimized all the structures relevant to the C−Cl reductive elimination process using the B97D/BS1 calculations. Single point calculations considering solvent effects were carried out for the structures obtained from B97D/BS1 using the M06/BS2//B97D/BS1 and B97D/BS2//B97D/BS1 levels of theories (see Figures S3 and S4 in the Supporting Information). Our results for X = Cl showed that the M06/BS2//M06/BS1 calculations reproduce the experimental data[2c] better than the other calculations. To this end, we have used only the energies calculated by M06/BS2//M06/BS1 with the inclusion of the solvent effects throughout the main text. The natural population analyses (NPA) and natural bond orbital (NBO) analyses on the bimetallic complexes were performed with the M06/BS3 level of theory.[14] BS3 uses the valence-triple-ξ basis set LANL2TZ(f) along with the corresponding ECP on Pd and the triple-ξ basis set 6-311G(d,p) on all remaining atoms. BS3 was used for these calculations to avoid the sensitivity of the population analyses to the presence of diffuse basis functions in BS2. In addition, it should be noted that although a similar trend in the population analyses is observed with BS1, we used BS3 to provide more reliable results. Two further basis sets containing diffuse d functions were explored for the NBO calculations, and they were found to give identical results to BS3 (see Supporting Information).

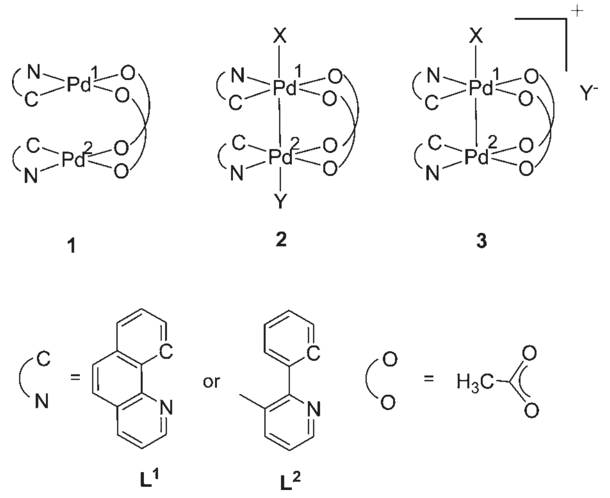

Figure 1. Intramolecular coordination for binuclear Pd(II) complexes (**1**) and higher oxidation states for palladium (**2**, **3**) illustrating typical ligand systems.

RESULTS AND DISCUSSION

To investigate reductive elimination to form a C-X bond from binuclear systems, we chose the model system **2** in which X is either Ph or Cl, Y is Cl, and C∼N is L^1 (Figure 1) for the DFT calculations. We also considered both CH_2Cl_2 and MeCN as solvents to ascertain the effect of solvent polarity. Direct and dissociative mechanisms need to be considered (Scheme 1). The possible pathway for direct reductive elimination is modeled on the mechanism reported for C−Cl reductive elimination from **2** (X = Y = Cl),[2c] and involves reductive elimination to form **4_X_Cl**, followed by dissociation of Cl from Pd^2 and its subsequent recoordination to Pd^1 to form **6_X_Cl**. Although our results for the direct reductive elimination are broadly in agreement with the previous computational study,[2c] the NBO and molecular orbital analyses undertaken here regarding the valence d orbitals uncover additional subtleties for the reductive elimination mechanism and for the structure and bonding of **4_X_Cl**. In particular, our additional analyses show that the direct C-X elimination from **2_X_Cl** to form **4_X_Cl** mainly involves reduction at Pd^1 leading to formulation of intermediate **4_X_Cl** as predominantly a Pd^1(I)-Pd^2(III) species.

For the dissociative pathway (Scheme 1), it is envisaged that Cl$^-$ may dissociate to form a cationic bimetallic species (**3_X**)

Scheme 1

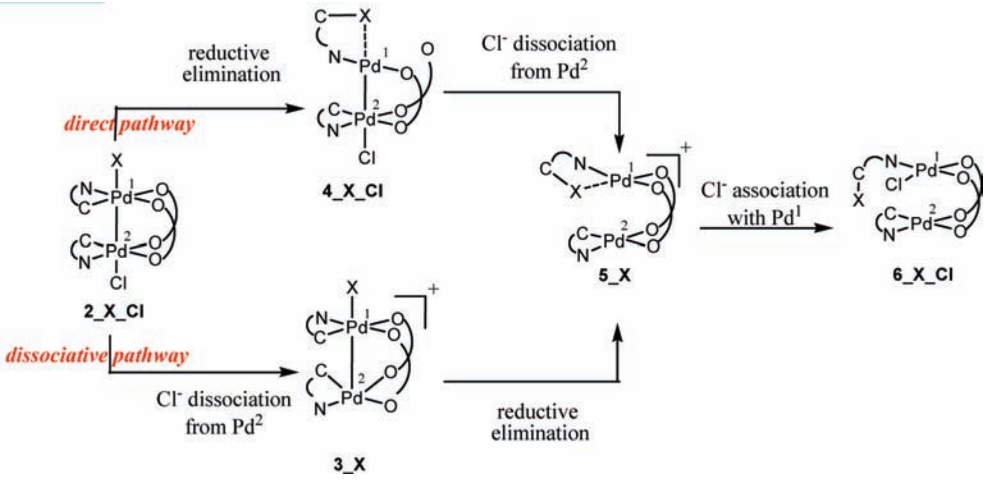

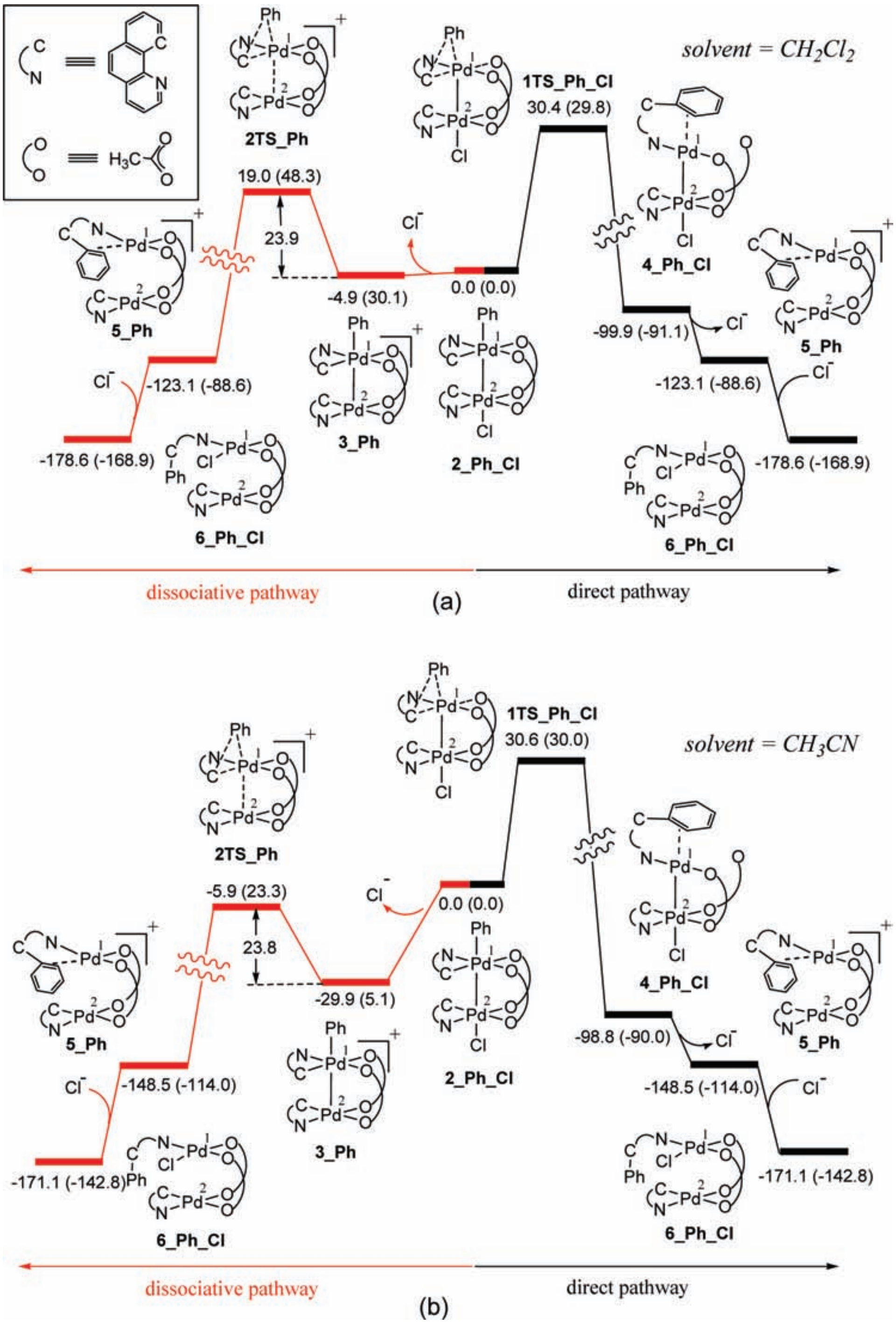

Figure 2. Energy profile for the direct and dissociative C-Ph reductive elimination in (a) CH_2Cl_2 and (b) MeCN. The calculated relative free energies (and enthalpies in parentheses) are given in kJ mol^{-1}.

that then undergoes reductive elimination and subsequent Cl^- recoordination.

For the phenyl system (**2**, X = Ph, Y = Cl), we find that the barrier for the direct pathway is higher than that for the dissociative pathway in both polar and nonpolar solvents (Figure 2).[12] This result is consistent with Sanford's proposal that reductive elimination occurs from bimetallic **3_Ph**.[3] For the chloride system (**2**, X = Y = Cl), our calculations suggest that the reductive elimination proceeds through the direct pathway when the solvent is of low polarity while in polar solvents the dissociative and direct pathways become competitive (Figure 3). This is supportive of Ritter's kinetic and reactivity studies in CH_2Cl_2[2] but suggests that caution is required in evaluating the role of this mechanism in other media such as polar solvents, a caveat generally acknowledged in mechanistic studies. It should be noted that the major difference between these two systems is related to the Pd^2—Cl bond strength and to solvation effects. When X = Ph, the Pd^2—Cl bond is weak, and the reaction proceeds through the dissociative pathway via **3_Ph** (Figure 2). On the other hand,

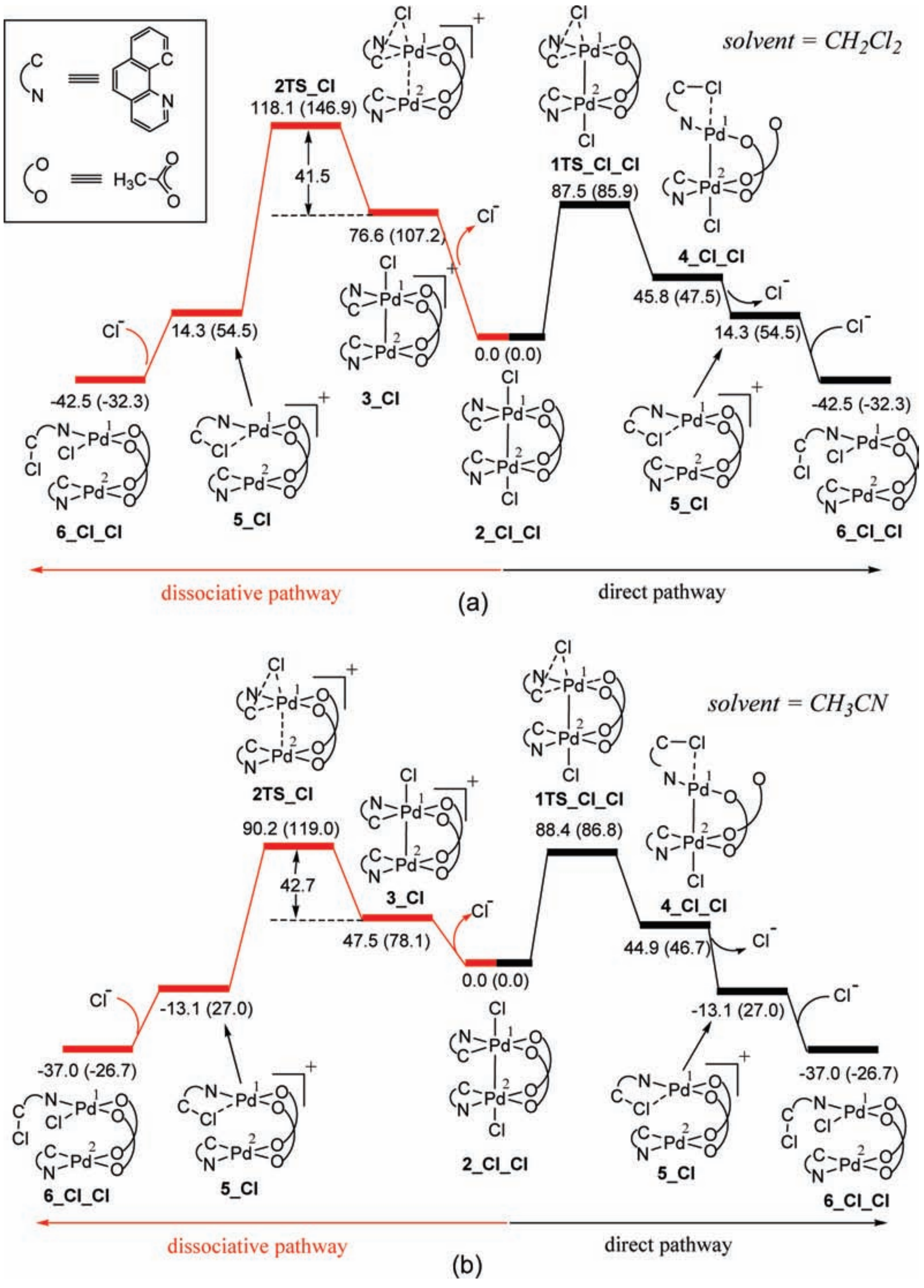

Figure 3. Energy profile for the direct and dissociative C−Cl reductive elimination in (a) CH_2Cl_2 and (b) MeCN. The calculated relative free energies (and enthalpies in parentheses) are given in kJ mol^{-1}.

when X = Cl, the Pd^2−Cl bond is stronger, and this diverts the reaction to a direct pathway, especially in CH_2Cl_2 solvent (Figure 3a). Our results also show that the direct reductive elimination barrier is relatively unaffected by solvent polarity, whereas the overall barrier in the dissociative pathway is strongly reduced by the more polar solvent. This difference can be explained by the higher stability induced by solvation of the charge separated species Cl^- and **3_X** by the more polar solvent during the initial chloride dissociation step.

Our calculations also reveal that the energy barrier for C-Ph reductive elimination is noticeably lower than for C−Cl reductive elimination in both solvents and for both direct and dissociative pathways, which can be related to the greater exothermicity for the formation of C-Ph bonds. The very low activation barrier calculated for the C-Ph coupling can also explain the fact that if **3_Ph** is formed during the catalytic reaction, as suggested by Deprez and Sanford,[3] it would immediately undergo the reductive elimination reaction. In other words, the most likely

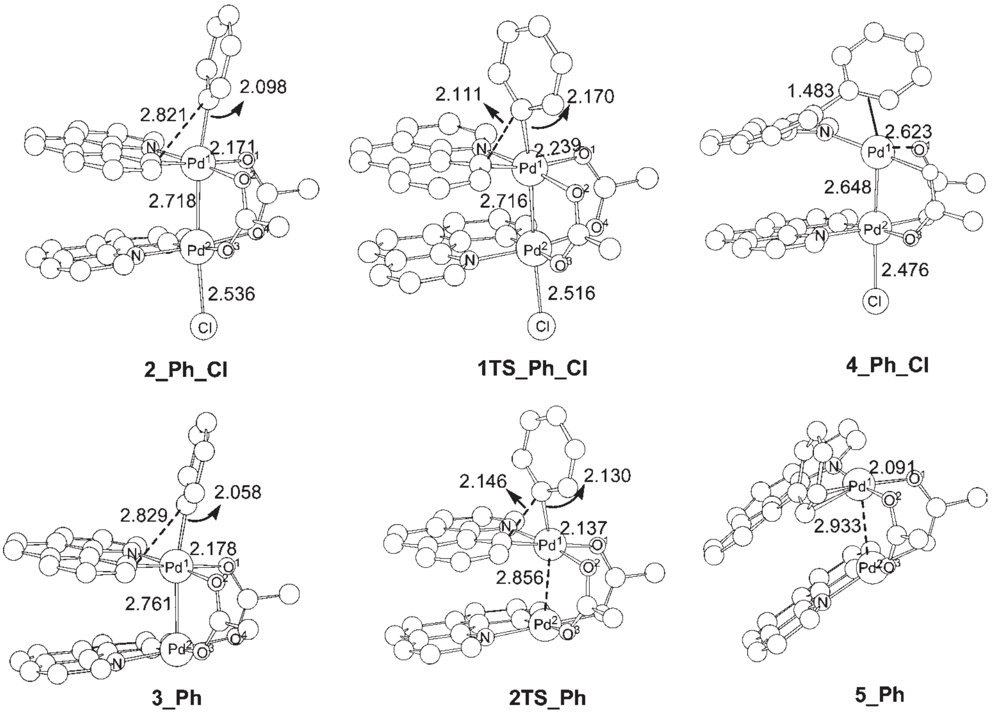

Figure 4. Calculated geometries for selected structures in the dissociative and direct reductive elimination pathways for X = Ph. Bond distances are given in Å. For clarity, the hydrogen atoms are omitted.

reason why **3_Ph** cannot be characterized experimentally is that it is very reactive toward the reductive elimination reaction.

Our calculations show that the reductive elimination from **3_X** occurs with a lower barrier than from **2_X_Cl** (Figures 2 and 3). This suggests that the electronic rearrangement mechanism of the reductive elimination process for these two species is probably different, a proposal supported by investigation of the structural parameters for the optimized structures in each pathway. Calculations show that the electronic rearrangement mechanism depends primarily on the pathway and less on the nature of the X ligand. To this end, we first compare the mechanisms of reductive elimination through the direct and dissociative pathways for X = Ph. Later on, we will discuss minor variations between X = Cl and X = Ph.

Electronic Rearrangement in the Reductive Elimination Reaction for 2 (X = Ph, Y = Cl) and 3 (X = Ph). Figure 4 shows the key structures for the direct and dissociative reductive elimination pathways for X = Ph. For direct reductive elimination from **2_Ph_Cl** to **4_Ph_Cl**, a progressive shortening of the Pd^1−Pd^2 and Pd^2−Cl bonds in conjunction with a Pd^1−O^1 bond lengthening is observed. In stark contrast, reductive elimination from **3_Ph** to **5_Ph** shows a reverse trend in bond lengths: the Pd^1−Pd^2 bond becomes longer and the Pd^1−O^1 bond becomes shorter. The d_{z^2} or $d_{x^2-y^2}$ orbitals on Pd^1 are both available to be populated by electrons during the course of the reductive elimination, and the mechanism of the reaction may be correlated with which of these is populated. A visual representation of the key d-orbital electron populations relative to **2_Ph_Cl** calculated by NBO for both pathways is shown in Figure 5. In the NBO calculations, the Pd^1−O^1, Pd^1−O^2, and Pd^1−Pd^2 bonds were considered as the *x*-, *y*-, and *z*-axes, respectively. (Details of the process of aligning the Cartesian coordinates to these axes are described in Supporting Information.) The relative values in Figure 5 show clearly that during direct reductive elimination the Pd^1 $d_{x^2-y^2}$ population increases steeply,[15] while the Pd^1 d_{z^2} population is relatively unchanged. Conversely, during the dissociative reductive elimination the $d_{x^2-y^2}$ population sharply decreases, while the Pd^1 d_{z^2} population increases dramatically.

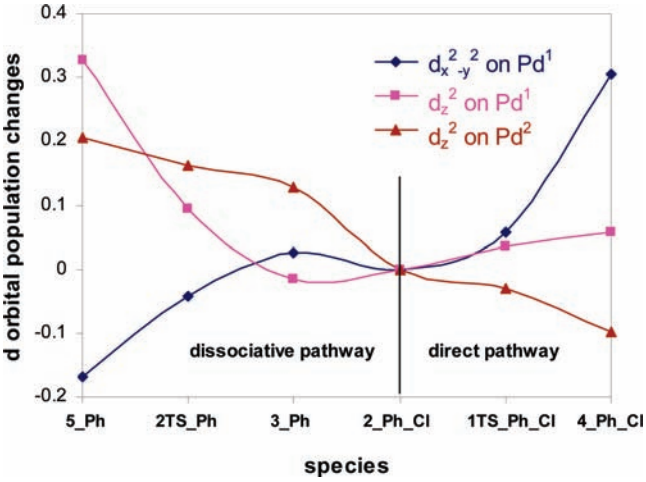

Figure 5. d-Orbital population changes relative to **2_Ph_Cl** for the dissociative and direct reductive elimination pathways.

This population trend is further confirmed by examining the molecular orbitals. The models show that, for both the direct (**2_Ph_Cl**, Figure 6) and dissociative pathways (**3_Ph**, Figure 7), the lowest unoccupied molecular orbital (LUMO) is predominantly d_{z^2} in character and is located on both the Pd^1 and Pd^2 centers, while the LUMO+1 is mainly $d_{x^2-y^2}$ based and is located only on Pd^1. The process of tilting the phenyl group of **2_Ph_Cl** toward the aryl group bound to Pd^1 and consequent C···C interaction, which leads to the formation of **4_Ph_Cl**, causes the LUMO+1 to drop in energy so that it becomes the highest occupied molecular orbital (HOMO) of

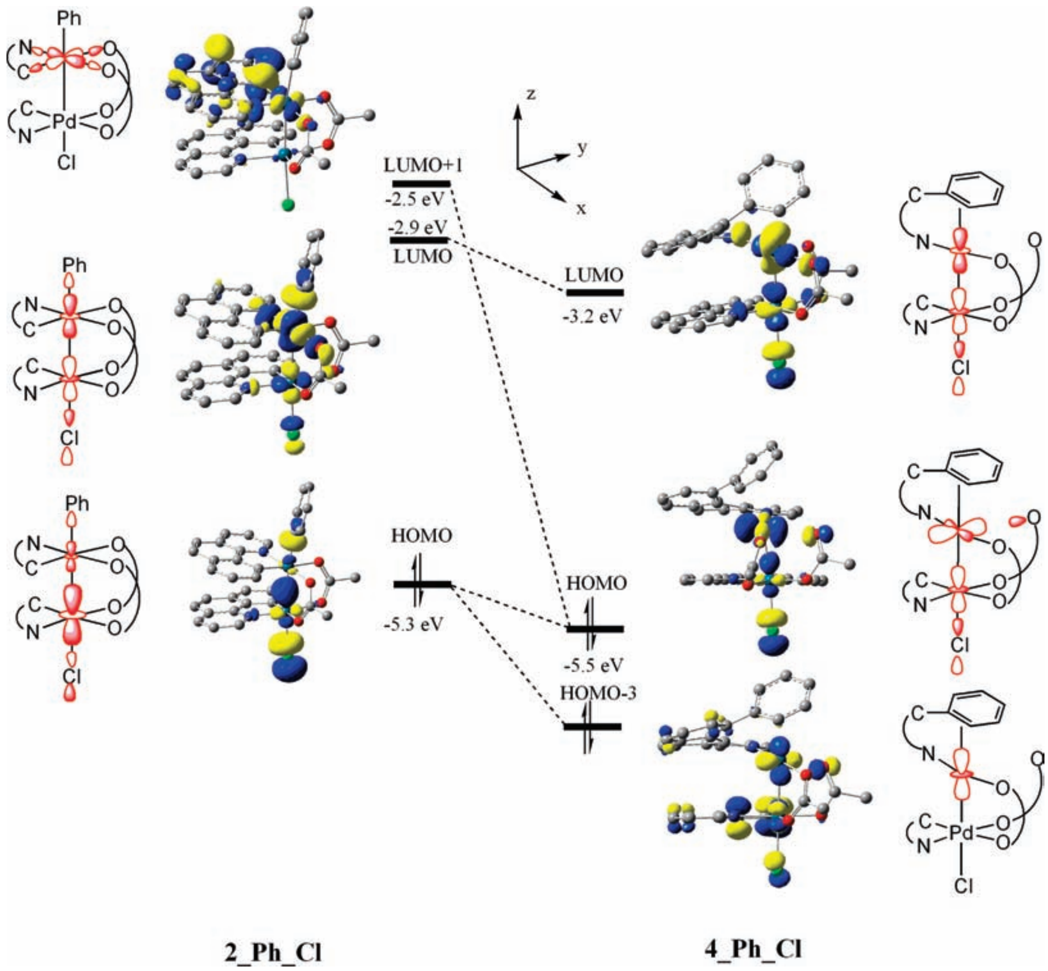

Figure 6. Correlation between the frontier molecular orbitals of **2_Ph_Cl** and **4_Ph_Cl** in the direct pathway.

4_Ph_Cl (Figure 6). In contrast, the analogous tilting process in **3_Ph** forces the lowest unoccupied molecular orbital (LUMO) to be populated, and gives the HOMO-1 in **5_Ph** (Figure 7). From these results, we can see that these pathways are differentiated on the basis of which of the orbitals is populated: the direct pathway populates the $d_{x^2-y^2}$ orbital located on Pd^1 while the dissociative pathway populates the d_{z^2} orbitals located on both Pd^1 and Pd^2.

In **2_Ph_Cl**, the LUMO suffers from an antibonding interaction between Cl and the Pd^2 d_{z^2} orbital (Figure 6). The presence of this antibonding interaction causes the LUMO to drop only slightly in energy as the departing groups are tilted toward each other and consequently this orbital remains intact. On the other hand, the reductive elimination process, which alleviates the $\sigma^*(C^1)$-$d_{x^2-y^2}(Pd^1)$ antibonding character in the LUMO+1 of **2_Ph_Cl**, lowers the energy of this orbital significantly, allowing it to be populated. This population, which is accompanied by $d_{x^2-y^2}$-s hybridization at Pd^1, results in a significant antibonding interaction between Pd^1 and O^1 (see HOMO for **4_Ph_Cl** in Figure 6). The consequence of this antibonding interaction is a considerable weakening of the Pd^1-O^1 bond. This result for the direct reductive elimination is consistent with a reduction in the formal oxidation state of Pd^1 from +3 in **2_Ph_Cl** toward +1 in **4_Ph_Cl**.

Oxidation State Changes of the Pd Metal Centers during Reductive Elimination through the Direct and Dissociative Pathways for 2 (X = Ph, Y = Cl). As noted above, the Pd−Pd and Pd^2-Cl bonds are shortened in going from **2_Ph_Cl** to **4_Ph_Cl** as the trans influence of phenyl is diminished. In this case, the electrons in the Pd^2 d_{z^2} orbital are polarized toward the Pd^1 d_{z^2} to reduce the Pd^2-Cl antibonding character in the HOMO of **2_Ph_Cl** (Figure 6). We find further support for this polarization in the observed changes in d orbital population (Figure 5), which show Pd^2 d_{z^2} population decreasing and Pd^1 d_{z^2} increasing slightly. This depopulation of the d_{z^2} orbital on Pd^2 in 4_Ph_Cl renders Pd^2 even closer to Pd(III) in character, consistent with occurrence of shorter Pd−Pd and Pd^2-Cl bonds.[16]

It follows from these results that the formal oxidation state of the Pd centers in **4_Ph_Cl** can be described as Pd^1(I)-Pd^2(III). The resulting geometry around Pd^2 is octahedral, while Pd^1 adopts a square planar geometry in the *xz* plane with one coordination site occupied by η^2-interaction with the phenyl group. However, dissociation of Cl^- from Pd^2 of **4_Ph_Cl** causes electron density to be significantly polarized along the *z* axis toward Pd^2, resulting in a change of formal oxidation state to Pd^1(II)-Pd^2(II) in **5_Ph**.

We now analyze the dissociative pathway for **2_Ph_Cl**. Following dissociation of chloride from **2_Ph_Cl**, there is an increase in polarization of electron density in **3_Ph** from the Pd^1 d_{z^2} orbital toward the Pd^2 d_{z^2} orbital (Figure 5). This suggests that Pd^2 in **3_Ph** is shifted toward the +2 oxidation state. This polarization assists in reducing the Pd^1-Ph antibonding

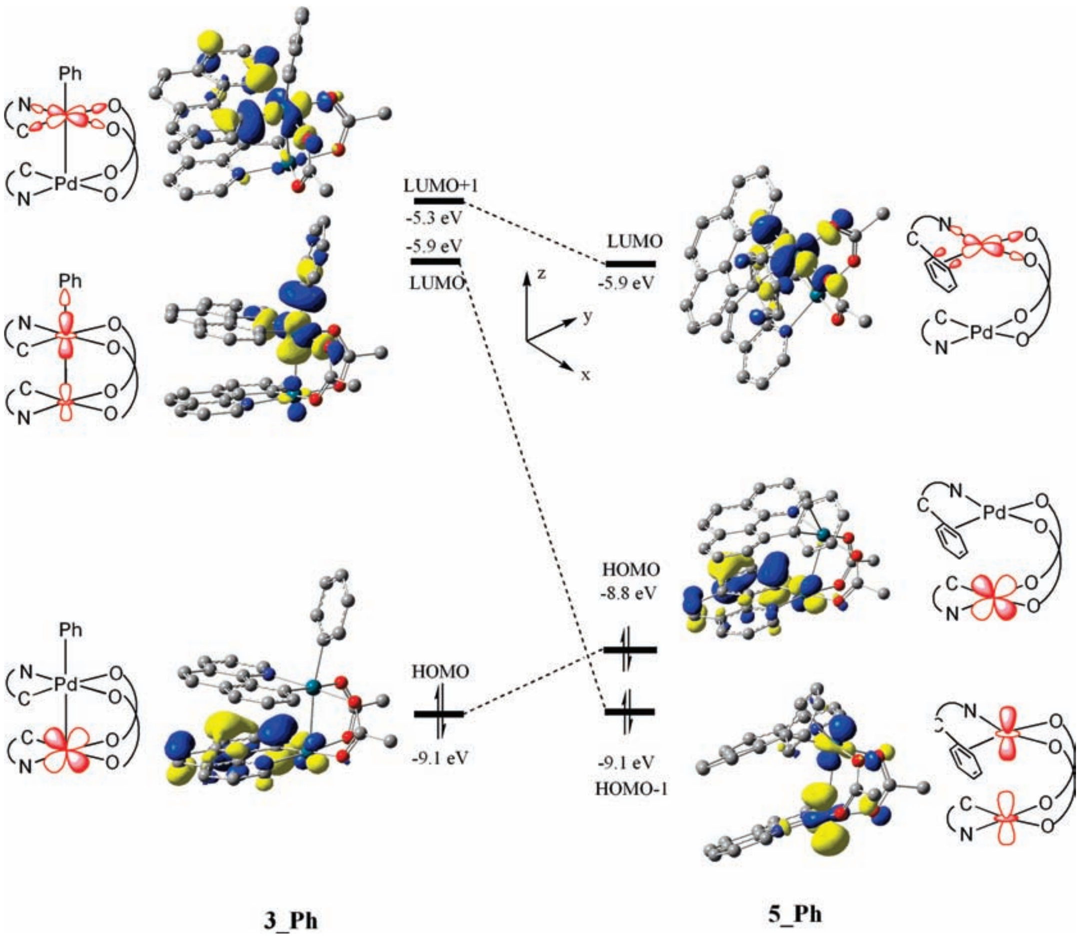

Figure 7. Correlation between the frontier molecular orbitals of **3_Ph** and **5_Ph** in the dissociative pathway.

interaction in the HOMO of **2_Ph_Cl**; the lessened antibonding interaction is reflected in a shorter Pd^1−Ph bond in **3_Ph** (2.058 Å) as compared to that in **2_Ph_Cl** (2.098 Å). The lengthening of the Pd^1−Pd^2 bond on going from **2_Ph_Cl** to **3_Ph** is also most likely a result of this polarization.[16]

In the reductive elimination step of the dissociative pathway, the key difference compared to the direct pathway is the absence of a Pd^2−Cl antibonding interaction in the LUMO of **3_Ph** causing this orbital to become populated during the reductive elimination, rather than the LUMO+1 (Figure 7). The increase in the Pd−Pd bond distance during the reductive elimination from **3_Ph** is thus a result of population of the d$_{z^2}$ orbitals involved in the antibonding interaction in the LUMO of **3_Ph**, as evidenced by the NBO calculation (Figure 5). This result suggests that the reductive elimination from **3_Ph** leads to a concomitant reduction of both Pd^1 and Pd^2. The concurrent shortening of the Pd^1−O^1 bond is then a result of the replacement of the strong σ-donor aryl moiety of the C∼N ligand in **3_Ph** with a weak π-donor interaction in the *xy* plane in **5_Ph**. This decrease in the σ-donating effect of the aryl ligand is reflected in the depopulation of the Pd^1 d$_{x^2-y^2}$ orbital from **3_Ph** to **5_Ph** (Figure 5).

As mentioned above, the reductive elimination from **2_X_Cl** has a higher energy barrier than **3_X**. Indeed, a corollary of the population of LUMO+1 in the reaction of **2_X_Cl** → **4_X_Cl** is that **1TS_X_Cl** undergoes a greater deformation than **2TS_X**, as evidenced by the shorter C^1−Ph bond in **1TS_X_Cl**. This suggests a later transition state for **1TS_X_Cl** than for **2TS_X**, which in turn leads to a higher activation barrier for the reaction of **2_X_Cl** → **4_X_Cl** than for the reaction of **3_X** → **5_X**.

Comparison of the Reductive Elimination Mechanism from 2_Ph_Cl and 2_Cl_Cl. As noted above, C-Ph reductive elimination from **2_Ph_Cl** via the dissociative mechanism leads to population of both Pd d$_{z^2}$ orbitals along with a depopulation of the d$_{x^2-y^2}$ orbital. In the analogous dissociative case for the Cl−C reductive elimination from **2_Cl_Cl** via **3_Cl**, the change in relative orbital populations follows the same pattern (Figure 8), and the variations of structural parameters for X = Cl (Figure 9) are very similar to those for X = Ph (Figure 4). Owing to an increase in population of both Pd d$_{z^2}$ orbitals, the Pd−Pd bond distance becomes longer on going from **3_Cl** to **5_Cl** (Figure 9).

In direct reductive elimination from **2_Ph_Cl**, the change of relative orbital populations differs from the dissociative process in that the Pd^1 d$_{x^2-y^2}$ orbital is populated while the Pd^2 d$_{z^2}$ orbital is depopulated. This population of the d$_{x^2-y^2}$ orbital is also observed for the direct Cl−C reductive elimination from **2_Cl_Cl** to form **4_Cl_Cl** (Figure 8), and is consistent with the longer Pd^1−O^1 distance in **4_Cl_Cl** (Figure 9). However, in contrast to **2_Ph_Cl**, a slight increase in the population of the Pd^2 d$_{z^2}$ orbital is observed (Figure 8). Replacement of the strong σ-donor Ph with Cl results in a covalent Pd−Pd bond for **2_Cl_Cl**. As a consequence, when the chloride departs from Pd^1 during the reductive elimination, the Pd^1 becomes more electron rich because of the change in oxidation state from

Pd(III) toward Pd(I), polarizing the electrons toward the Pd^2 d$_{z^2}$ orbital. This increase in population of the Pd^2 d$_{z^2}$ orbital is then reflected in the elongated Pd^2−Cl bond in **4_Cl_Cl** (Figure 9).[16] This result also shows that, in comparison with the oxidation state Pd(III) in **2_Cl_Cl**, the oxidation state of Pd^2 in **4_Cl_Cl** is shifted a little toward Pd(II).

As noted earlier, our results for the direct pathway for C−Cl bond formation from **2_Cl_Cl** are in broad agreement with the initial computational study.[2c] In particular there is good agreement in both the geometries and the trends in geometries for species in the sequence **2_Cl_Cl** to **6_Cl_Cl**. A difference does occur in the relative orientation of the chelate rings of Pd^1 and Pd^2 in three structures, illustrated by N−Pd−Pd−N dihedral angles for **2_Cl_Cl** (61.8, 102.3°), **1TS_Cl_Cl** (65.0, 101.7°), and **4_Cl_Cl** (63.9, 97.3°), where the lower value in each case refers to the present work. The lower values are similar to the value for the crystal structure of **2_Cl_Cl** (60.67°).[2c,17a] The studies differ in interpretation for **4_Cl_Cl**. The initial report involved calculation of electron binding energies of the 4s electrons of Pd^1 and Pd^2, for which monotonic decreases for Pd^1 and Pd^2 were interpreted in terms of a model with a steady transition from Pd^{III}−Pd^{III} in **2_Cl_Cl** to Pd^{II}−Pd^{II} in the products. This approach is consistent with recent practice, as noted in the previous report, although we are unaware of any reports that it is appropriate for complex systems involving metal−metal bonding. The approximate Pd^1(I)-Pd^2(III) interpretation for **4_Cl_Cl** herein is based upon NBO calculations,[17b] in particular increased population of d$_{x^2-y^2}$ at Pd^1 on going from **2_Cl_Cl** to **4_Cl_Cl** resulting in a formal approximate oxidation state assignment based upon the classical approach of consideration of valence shell electron configurations. This interpretation is consistent with computed geometries obtained in both studies: lengthening of the Pd^1−O distance, and shortening of Pd^1−Pd^2 indicative of a sustained metal−metal interaction that would, rather simplistically, be anticipated for a formal "d^9-d^7" configuration. Thus, with regard to direct elimination for **2_Cl_Cl**, the present study builds directly upon the initial report,[2c] is in general agreement on the structures of intermediates, and provides additional interpretation as a result of NBO calculations.

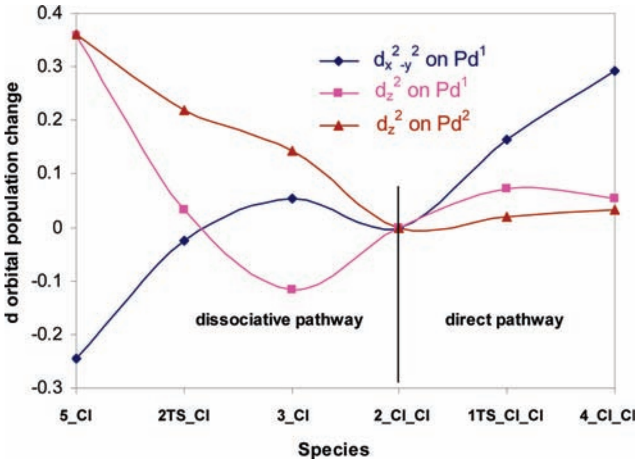

Figure 8. d-Orbital population changes relative to **2_Cl_Cl** for the dissociative and direct reductive elimination pathways.

■ CONCLUSIONS

DFT calculations were performed to investigate the mechanism of formation of C−Cl and C−C bonds via reductive elimination from binuclear organopalladium complexes [(L-*C*,*N*)XPd^1-(μ-O$_2$CMe)$_2$Pd^{2}Cl(L-*C*,*N*)], **2**, through a dissociative and a direct pathway. For X = Cl, this study refers to an isolated complex demonstrated to undergo facile C−Cl bond formation as part of a seminal investigation of organopalladium(III) chemistry;[2a,b] while for X = Ph and dissociated Cl, the calculations serve as a model for a

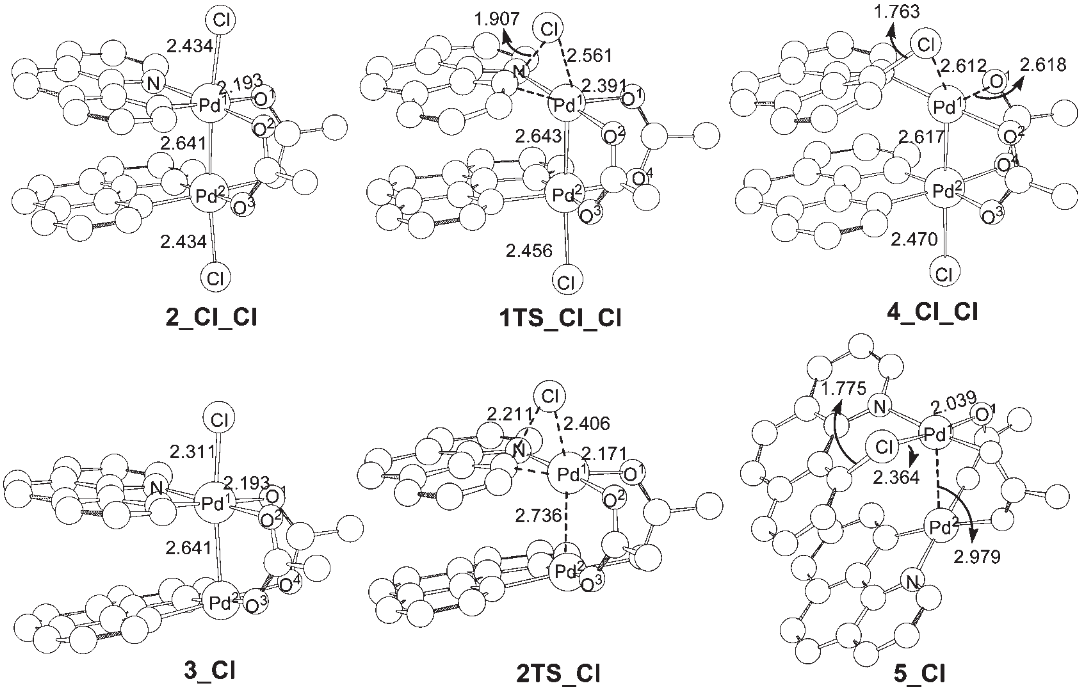

Figure 9. Calculated geometries for selected structures in the dissociative and direct reductive elimination pathways for X = Cl. Bond distances are given in Å. For clarity, the hydrogen atoms are omitted.

proposed pathway for C−C bond formation from a cation and thus, while indicating that reductive elimination is feasible from this cation, do not provide direct confirmation of the proposal for catalysis.[3] In the direct pathway, reductive elimination occurs from **2** followed by dissociation of Cl^- from Pd^2 and its subsequent recoordination to Pd^1. However, in the dissociative pathway, loss of Cl^- yields the cationic bimetallic species $[(L\text{-}C,N)XPd^1\text{-}(\mu\text{-}O_2CMe)_2Pd^2(L\text{-}C,N)]^+$, **3**, which undergoes reductive elimination and then subsequent Cl^- recoordination to Pd^1. Several important conclusions can be drawn from the results of the calculations:

(1) For bimetallic complexes **2** where X = Ph the dissociative pathway is more favorable regardless of the solvent polarity (because of the very weak Pd^2−Cl bond in **2**).

(2) For bimetallic complexes **2** where X = Cl the direct pathway is more favorable when a low polarity solvent is used, while in high polarity solvents the dissociative pathway becomes competitive (because of solvation of the charged species).

(3) The direct pathway proceeds via transferring two electrons from the departing groups to the Pd^1 $d_{x^2-y^2}$ orbital (LUMO+1 in **2**) providing an approximate Pd^1(I)-Pd^2(III) mixed oxidation state system. Subsequent Cl^- dissociation results in electron-polarization from Pd^1 to Pd^2 giving a Pd(II),Pd(II) system.

(4) In the dissociative pathway, the reductive elimination occurs with electron-transfer into the d_{z^2} orbitals on Pd^1 and Pd^2 (LUMO in **3_X**). This process leads to the breaking of the Pd^1−Pd^2 bond, and concomitant change of oxidation state from Pd(III)−Pd(III) to Pd(II),Pd(II).

(5) The reductive elimination step from the neutral bimetallic complex **2** is more difficult than from the cationic bimetallic complex **3**. This is because the process of populating the LUMO+1 in the direct reductive elimination from **2** requires greater deformation energy.

ASSOCIATED CONTENT

Supporting Information. Complete ref 4, additional information regarding the NBO calculations, Cartesian coordinates of all optimized structures. This material is available free of charge via the Internet at http://pubs.acs.org.

AUTHOR INFORMATION

Corresponding Author

*E-mail: Allan.Canty@utas.edu.au (A.J.C.), Brian.Yates@utas.edu.au (B.F.Y.). Fax: (61-3) 6226-2858.

ACKNOWLEDGMENT

We thank the Australian Research Council for financial support, and the Australian National Computational Infrastructure and the University of Tasmania for computing resources.

REFERENCES

(1) Ariafard, A.; Hyland, C. J. T.; Canty, A. J.; Sharma, M.; Brookes, N. J.; Yates, B. F. *Inorg. Chem.* **2010**, *49*, 11249−11253.

(2) (a) Powers, D. C.; Ritter, T. *Nat. Chem.* **2009**, *1*, 302. (b) Powers, D. C.; Geibel, M. A. L.; Klein, J. E. M. N.; Ritter, T. *J. Am. Chem. Soc.* **2009**, *131*, 17050. (c) Powers, D. C.; Benitez, D.; Tkatchouk, E.; Goddard, W. A., III; Ritter, T. *J. Am. Chem. Soc.* **2010**, *132*, 14092.

(3) Deprez, N. R.; Sanford, M. S. *J. Am. Chem. Soc.* **2009**, *131*, 11234.

(4) Frisch, M. J. et al. *Gaussian 09*, revision A.02; Gaussian, Inc.: Wallingford, CT, 2009.

(5) (a) Zhao, Y.; Schultz, N. E.; Truhlar, D. G. *J. Chem. Theory Comput.* **2006**, *2*, 364. (b) Zhao, Y.; Truhlar, D. G. *J. Chem. Phys.* **2006**, *125*, 194101. (c) Zhao, Y.; Truhlar, D. G. *J. Phys. Chem. A* **2006**, *110*, 13126.

(6) (a) Sieffert, N.; Bühl, M. *Inorg. Chem.* **2009**, *48*, 4622. (b) Benitez, D.; Tkatchouk, E.; Goddard, W. A., III. *Organometallics* **2009**, *28*, 2643. (c) Benitez, D.; Shapiro, N. D.; Tkatchouk, E.; Wang, Y. M.; Goddard, W. A., III.; Toste, F. D. *Nat. Chem.* **2009**, *1*, 482.

(7) (a) Hay, P. J.; Wadt, W. R. *J. Chem. Phys.* **1985**, *82*, 270. (b) Wadt, W. R.; Hay, P. J. *J. Chem. Phys.* **1985**, *82*, 284. (c) Roy, L. E.; Hay, P. J.; Martin, R. L. *J. Chem. Theory Comput.* **2008**, *4*, 1029.

(8) Hariharan, P. C.; Pople, J. A. *Theor. Chim. Acta* **1973**, *28*, 213.

(9) Ehlers, A. W.; Böhme, M.; Dapprich, S.; Gobbi, A.; Höllwarth, A.; Jonas, V.; Köhler, K. F.; Stegmann, R.; Veldkamp, A.; Frenking, G. *Chem. Phys. Lett.* **1993**, *208*, 111.

(10) Weigend, F.; Furche, F.; Ahlrichs, R. *J. Chem. Phys.* **2003**, *119*, 12753.

(11) Barone, V.; Cossi, M. *J. Phys. Chem. A* **1998**, *102*, 1995.

(12) In dissociation of neutral ligands (e.g., PMe_3) from organometallic complexes, it has been shown that the calculated ΔH for the overall dissociation reaction is a good estimate of $\Delta G^\ddagger$ for the dissociation barrier: Wei, C. S.; Jiménez-Hoyos, C. A.; Videa, M. F.; Hartwig, J. F.; Hall, M. B. *J. Am. Chem. Soc.* **2010**, *132*, 3078. However in the dissociations considered here involving charge separated species, it is more appropriate to consider the calculated ΔG for the overall dissociation reaction when constructing the relative energy profiles.

(13) (a) Grimme, S. *J. Comput. Chem.* **2004**, *25*, 1463. (b) Grimme, S. *J. Comput. Chem.* **2006**, *27*, 1787.

(14) Glendening, E. D.; Read, A. E.; Carpenter, J. E.; Weinhold, F. *NBO*, version 3.1; Gaussian, Inc.: Pittsburgh, PA, 2003.

(15) Only a negligible increase in the population of the Pd^2 $d_{x^2-y^2}$ orbital is observed on going from **2_Ph_Cl** (1.247) to **4_Ph_Cl** (1.272) indicating that the Pd^2 $d_{x^2-y^2}$ orbital is not involved in the electron transfer process of the direct reductive elimination from **2_Ph_Cl**.

(16) In a recent study (ref 1), we have shown that there is a good correlation between the population of the Pd^2 d_{z^2} orbital and the Pd^2−Cl bond distance. Indeed, as the population of the d_{z^2} Pd^2 orbital increases, Pd^2 becomes closer to the +2 oxidation state. We have also indicated that the Pd−Pd bond distance is affected by both the X and Y trans influence and the Pd^2 oxidation state. The stronger the X (or Y) trans influencing ligand, the longer the Pd−Pd bond. The closer the oxidation state of Pd^2 to Pd(II), the longer the Pd−Pd bond.

(17) (a) Our structure **2_Cl_Cl** is a rotational conformer of Structure **A** reported in ref 2c. Our structure corresponds to the conformation found in the crystal structure and is more stable than Structure **A** by about 6 kJ/mol at the optimization level of theory. Similarly **1TS_Cl_Cl** and **4_Cl_Cl** are more stable by 5−6 kJ/mol than the corresponding structures **B** and **C** in ref 2c. See Supporting Information. (b) Structures **A**−**E** in ref 2c give identical NBO results to our analogues (See Supporting Information).